KI REPORTS
KIReports.org

Modelling X-linked Alport Syndrome With Induced Pluripotent Stem Cell-Derived Podocytes

Ricky Wai Kiu Lau[1], Craig Fisher[1], Thanh Kha Phan[2], Dilara Ceyda Ozkocak[2], James Selby[3], Sheetal Saini[1], Sarvatha Mukundan[1], Andrea F. Wise[1], Judith Savige[4], Ivan Ka Ho Poon[2], John Haynes[3] and Sharon D. Ricardo[1]

[1]Department of Pharmacology, Biomedicine Discovery Institute, Monash University, Clayton, Victoria, Australia; [2]Department of Biochemistry, La Trobe Institute for Molecular Science, La Trobe University, Victoria, Australia; [3]Monash Institute of Pharmaceutical Sciences, Monash University, Parkville, Victoria, Australia; and [4]The University of Melbourne, Parkville, Victoria, Australia

Correspondence: Sharon D. Ricardo, Department of Pharmacology, Biomedicine Discovery Institute, Monash University, 9 Ancora Imparo Way, Clayton, Victoria, 3800 Australia. E-mail: sharon.ricardo@monash.edu

Kidney Int Rep (2021) **6,** 2912–2917; https://doi.org/10.1016/j.ekir.2021.07.027

KEYWORDS: Alport syndrome; chaperone; endoplasmic reticular stress; induced pluripotent stem cells; podocytes

Alport syndrome is caused by mutations in the collagen type IV alpha 3-5 (*COL4A3-5)* genes, resulting in glomerular basement membrane abnormalities and podocyte depletion.[1] Angiotensin II (AngII) promotes podocyte depletion through a complex cascade of profibrotic cell signalling via inappropriate integrin-cell interaction with the glomerular basement membrane, leading to abnormal cytoskeleton organization and apoptosis.[2] The progression of podocyte damage results in foot process effacement and proteinuria.[3] Transient receptor potential channel 6 and elevated AngII are associated with podocyte injury in Alport syndrome and many other podocytopathies.[4]

Nevertheless, podocyte research has been hampered by the lack of suitable models for defining factors regulating podocyte survival and function. Primary cultures of human podocytes only replicate for a short time, and cannot be maintained over long periods.[5] Additionally, most *in vitro* research has been conducted using immortalized podocytes (IMM-PODs), which are limited to a single genetic background and limited differentiation capacity.[6] Induced pluripotent stem cells (iPSCs) using adult cell reprogramming[7] provide an unprecedented opportunity to elucidate disease mechanisms *in vitro* and provide tools for understanding genetic disease by decoding genotype-to-phenotype correlation.[8] Kidney podocytes generated through the directed differentiation of iPSCs (iPSC-PODs), maintain podocyte characteristics comparable to IMM-PODs or primary podocytes.[9,S10,S11] Therefore, the differentiation of iPSCs from Alport syndrome patients[S12] provides a long-term and self-renewing strategy to study X-linked Alport syndrome.

The precise molecular mechanism underlying X-linked *COL4A5* mutations promoting Alport syndrome remains unclear. Podocyte depletion through apoptosis in Alport syndrome may result from an overexpression of tumour necrosis factor alpha (TNF-α),[2] produced by infiltrating macrophages, or possibly from elevated reabsorption of protein in proximal tubular epithelial cells.[3] In Alport syndrome, the accumulation of misfolded proteins in podocyte rough endoplasmic reticulum (RER) may induce the unfolded-protein response for missense mutations.[S13] Pathological endpoints of RER stress include podocyte apoptosis and autophagy due to defective localization of *COL4A5*.[S14] There is growing interest in the therapeutic use of chaperones for treating inherited renal disease. The protein-folding chaperone, 4-phenylbutyric acid (PBA) can reduce RER size by resolving the aggregation of the misfolded cytoplasmic collagen matrix.[S15,16] The elucidation of how gene *COL4A5* mutations cause podocyte injury is a fundamental step for future studies to improve disease outcomes.

This study compares iPSCs derived from a male patient with X-linked Alport syndrome due to a *COL4A5* missense mutation (*p.G624D*) to wild-type (WT) control

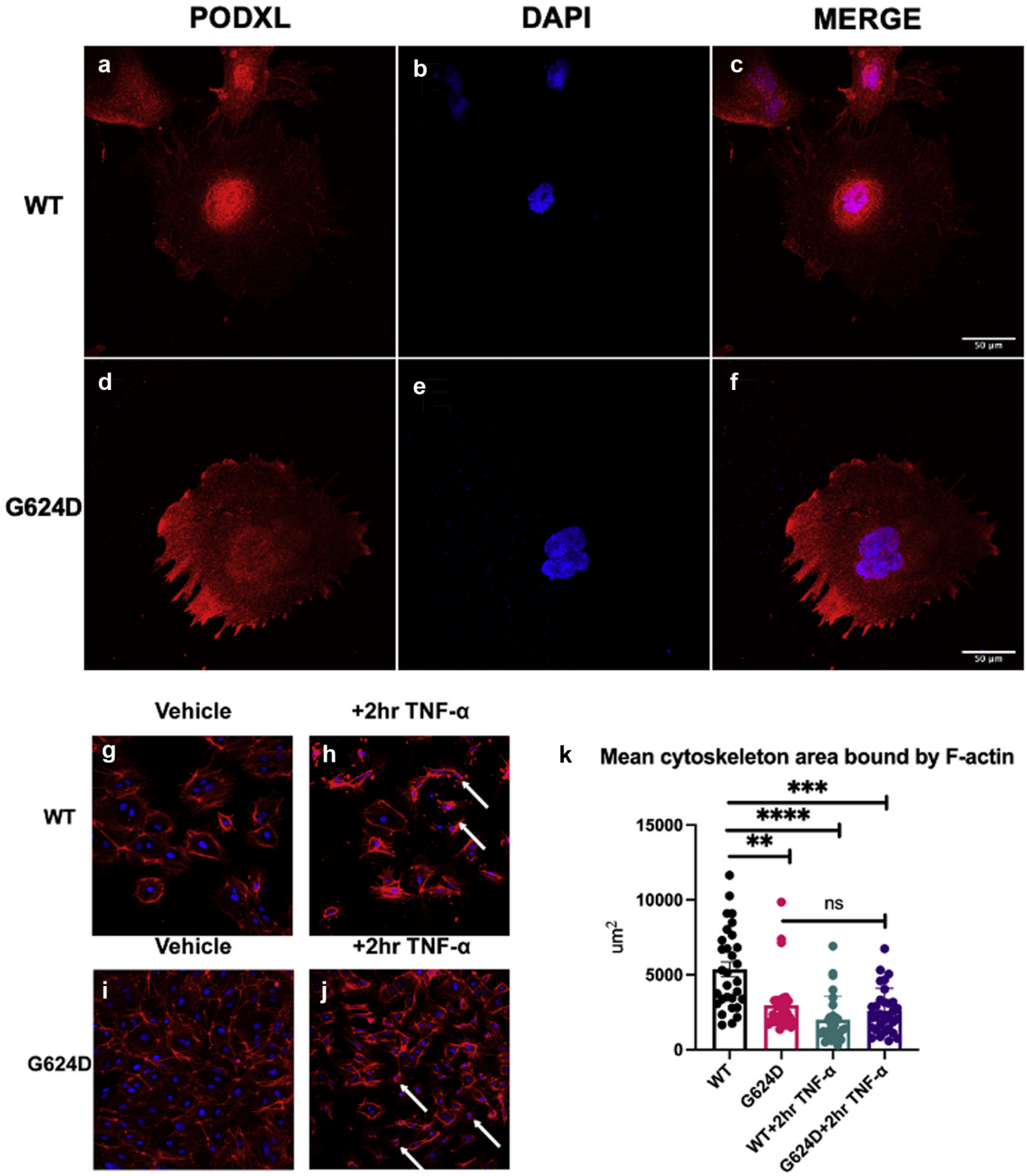

Figure 1. Differentiation of G624D induced pluripotent stem cells (iPSCs) into iPSC podocytes (PODs) and F-actin cytoskeletal arrangement in response to tumor necrosis factor alpha (TNF-α). **(a-c)** Wild-type (WT) iPSC-PODs expressed podocyte specific markers such as PODXL in the cytoplasm, also observable in **(d-f)** G624D iPSC-PODs. Confocal images of F-actin labelled **(g, h)** WT and **(i, j)** G624D iPSC-PODs before and after TNF-α induced cell death. Differences were found in the F-actin cytoskeletal arrangement between WT and G624D D10 iPSC-PODs, seeded at the same cell density. Two-hour treatment of TNF-α caused cell death and podocyte detachment **(arrows)** in both WT and G624D iPSC-POD D10 (original magnifications ×20). **(k)** Quantification of the mean cell area showed that G624D iPSC-POD D10 exhibited a significantly smaller mean cell area than WT. TNF-α caused a significant reduction in mean cell area in WT, but had less influence on the cytoskeleton rearrangement in G624D. N = 3 to 5; 5 fields; All data were presented as mean + SEM.

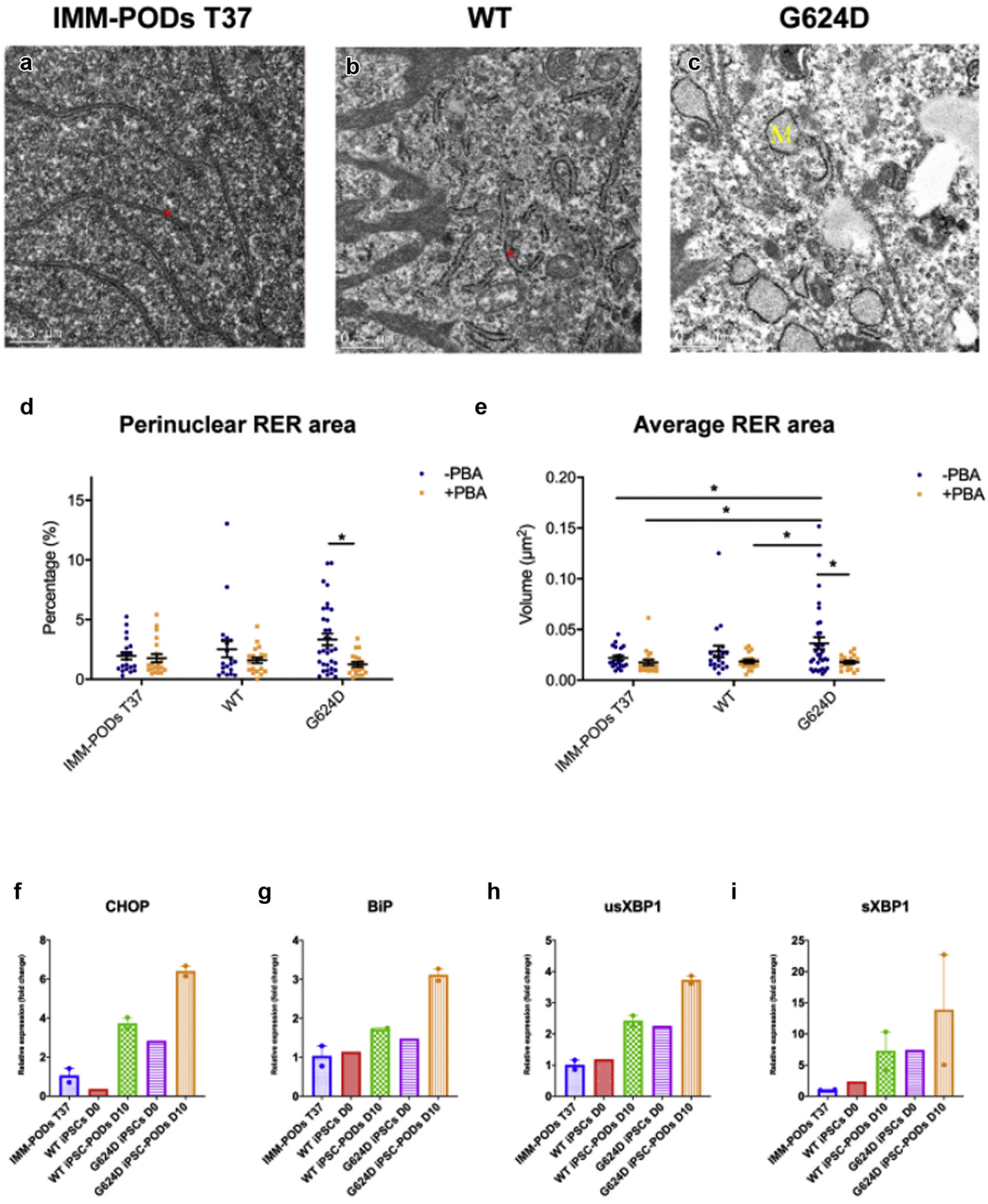

Figure 2. Dysregulated rough endoplasmic reticulum (RER) was found exclusively in G624D induced pluripotent stem cell (iPSCs)–podocyte (POD) D10 and the treatment of 4-phenylbutyric acid (PBA) reduced the RER enlargement. Representative images of transmission electron microscopy analysis are shown as **(a)** immortalized (IMM)–PODs T37, **(b)** wild-type (WT), and **(c)** G624D iPSC-PODs D10. IMM-PODs T37 and WT iPSC-PODs D10 (Red dot showing luminal widths) did not show any abnormality in the RER. Enlarged RER organelle (Yellow *M*) was found in G624D iPSC-PODs D10. **(d)** Quantification of perinuclear RER percentage area revealed differences in mean area of cell lines (n = 20). However, PBA treatment was shown to reduce the total perinuclear RER percentage area of G624D iPSC-PODs ($P = 0.0021$), not statistically significant in IMM-POD and WT controls (original magnification, ×40,000; scale bars: 0.5 µm). **(e)** Average RER volume was also taken as a factor of the number of RER units in a perinuclear location. Supplementary treatment with PBA again reduced the average RER volume to significant differences in the G624D ($P = 0.0332$). Two-way analysis of variance with Tukey's *post hoc* test. All data were presented as mean ± SEM. The gene expression of endoplasmic reticulum stress markers **(f)** CHOP, **(g)** BiP, **(h)** usXBP1, and **(i)** sXBP1 were quantified using quantitative polymerase chain reaction. Following 10 days after differentiation, G624D iPSC-PODs showed an upregulated mRNA expression of endoplasmic reticulum stress markers, CHOP, BiP, uSXBP1, and sSXBP1 compared to WT iPSC-POD controls.

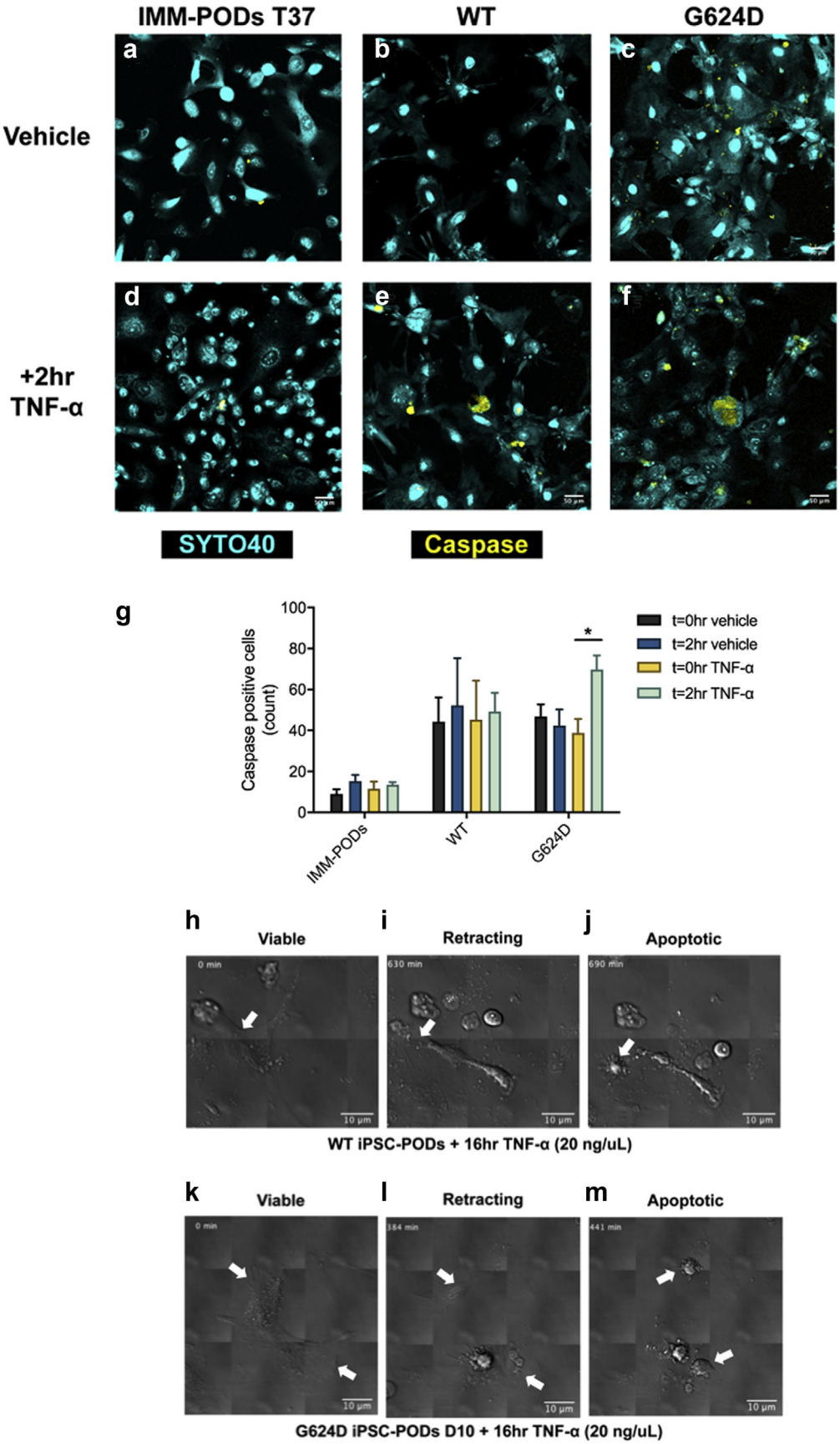

Figure 3. G624D displayed increased susceptibility to tumor necrosis factor alpha (TNF-α)–stimulated podocyte death after 2-hour TNF-α exposure. Representative images of the vehicle and after a 2-hour treatment with media containing 20 ng/ml TNF-α are shown for (**a** and **d**) immortalized (IMM)–podocytes (PODs), (**b** and **e**) wild-type (WT), and (**c** and **f**) G624D induced pluripotent stem cells (iPSC)–PODs. (Continued)

subjects presenting with normal renal function. Pluripotency was confirmed in WT and Alport G624D iPSCs before the directed differentiation into podocytes.[9] Cell ultrastructure of iPSC-PODs was assessed using transmission electron microscopy and chaperone treatment using PBA was found to have a protective effect on Alport iPSC-PODs by reducing the size of dysregulated RER due to protein accumulation. Increased endoplasmic reticulum stress genes encoding for Binding immunoglobulin protein (BiP), CCAAT/enhancer-binding protein homologous protein (*CHOP*) and X-box binding protein 1 (*XBP1*) were upregulated in Alport iPSC-PODs D10 comparing to WT iPSC-PODs. Furthermore, Alport iPSC-PODs were more susceptible to TNF-α–mediated apoptosis, and an elevated intracellular calcium influx (caused by AngII) when compared to WT controls. Taken together, we provide evidence that Alport iPSCs maintain genotype-phenotype correlations to explore patient-relevant cellular mechanisms targeted for therapeutic development.

METHODS

See Supplementary Methods.

RESULTS

Dermal skin fibroblasts outgrowths were cultured from an Alport patient with the hemizygous X-linked *COL4A5* missense mutation, *p.G624D* in exon 46 (G624D),[S16] which is common in Europe, accounting for approximately 40% of the cases in Poland. Primary fibroblast outgrowths were desmin-positive with COL4A5 protein expression localized in a perinuclear pattern (Supplementary Figure S1). The fibroblasts were transduced into iPSCs using nonintegrating Sendai virus reprogramming. The iPSC colonies were alkaline phosphatase-positive and expressed the pluripotency markers: OCT4, SSEA4, TRA-1-60, and TRA-1-81. Moreover, Alport syndrome iPSC colonies retained *COL4A5* expression, analogous to primary fibroblasts (Supplementary Figure S1). Undifferentiated Alport G624D iPSCs that were karyotypically normal were engrafted under the kidney capsule of nonobese diabetic–severe combined immunodeficiency mice confirming teratoma formation after 12 weeks (Supplementary Figure S1). Both WT and G624D iPSCs were differentiated into iPSC-PODs as previously reported[S12] that expressed PODXL, a mature podocyte marker (Figure 1). There was a significant difference in F-actin organization, measured as mean cell size as defined by F-actin between control WT and G624D Alport iPSC-PODs following TNF-α stimulation (Figure 1).

DISCUSSION

Previously, we reported that the chaperone PBA alleviated accumulated misfolded protein in the endoplasmic reticulum of Alport fibroblasts, expressing COL4A3, 4, and 5.[S16] Therefore, PBA was added to G624D Alport iPSC-PODs to determine the effectiveness to attenuate misfolded RER COL4A5 protein. By transmission electron microscopy, the RER of G624D Alport iPSC-PODs appeared dilated and enlarged (Yellow *M*; Figure 2) compared to WT and IMM-PODs (Red dots; Figure 2). The addition of PBA reduced both the perinuclear and average RER area of the Alport iPSC-PODs compared to WT and IMM-POD controls. Using quantitative polymerase chain reaction, there was an upregulation of endoplasmic reticulum stress markers: *CHOP*, *BiP* and unspliced *XBP1* (*usXBP1*) and spliced *XBP1* (*sXBP1*) in G624D Alport iPSC-PODs after 10 days of differentiation, compared to WT iPSC-PODs (Figure 2).

Alport iPSC-POD susceptibility to TNF-α–mediated apoptosis was also investigated. WT, G624D iPSC-PODs, and IMM-PODs were exposed to TNF-α for 2 hours to stimulate podocyte injury (Figure 3). Importantly, only G624D iPSC-PODs displayed a significant increase in caspase-positive cells correlating with cell death over 2 hours (38.8 ± 6.9 cells vs. 69.8 ± 6.9 cells; P=0.0332), compared to baseline (Figure 3). This indicated an increased susceptibility of G624D Alport iPSC-PODs to TNF-α–stimulated apoptosis compared to WT and IMM-PODs without the *COL4A5* mutation.

Differential interference contrast microscopy was used to visualize D10 G624D Alport and WT iPSC-PODs to examine the susceptibility to cell death over an extended period of TNF-α exposure for 16 hours (Figure 3). The assessment of time-lapsed, live-cell imaging in Alport

Figure 3. (Continued) **(g)** All cell lines (n = 4) were analyzed for the presence of caspase-positive cells using the caspase inhibitor VAD-FMK conjugated to sulfo-rhodamine (Red-VAD-FMK) as the fluorescent *in situ* marker. Comparisons within cell lines outlined increased caspase positive cells in the G624D iPSC-PODs after the 2-hour TNF-α exposure ($P < 0.05$) compared to t = 0. The other two cells displayed trends of increased caspase positive cells after 2 hours regardless of vehicle or TNF-α treatment without significant differences. All data were compared by one-way analysis of variance with Tukey's *post hoc* test form comparisons made only within cell lines with/without TNF-α treatment. All data were presented as mean ± SEM. Differential interference contrast microscopy was performed to assess the susceptibility of the diseased iPSC-PODs to retraction and cell death following the addition of TNF-α over 16 hours of culture. In **(h-j)** WT iPSC-PODs, cell blebbing, and retraction, which represent morphological hallmarks of apoptosis, were observed at ~600 minutes, compared to **(k-m)** G624D iPSC-POD D10, at ~360 minutes. The time-lapse imaging provided evidence that G624D iPSC-PODs D10 displayed apoptotic morphology and were more susceptible to early-onset cell death compared to WT cells.

iPSC-PODs, compared to WT iPSC-PODs (Figure 3), shows the retraction of podocytes and evidence that podocytes displayed apoptotic morphology (including membrane blebbing) earlier in disease cells compared to WT cells (Supplementary Movies S1 and S2).

In a previous study, we showed that AngII promotes concentration-dependent elevations of intracellular calcium that were particularly sensitive to the AngII type-1 receptor antagonist, losartan.[S12] In this study, we performed an AngII responsiveness assay on WT and G624D Alport iPSC-PODs D10 following 24-hour stimulation of TNF-α (Supplementary Figure S2). The increase in 340/380 emission ratio indicated the binding of more cytosolic free Ca^{2+} to FURA-2 AM, a Ca^{2+} fluorescent indicator. As a result, the excitation wavelength changed from 380 nm to 340 nm; the increase in 340/380 emission ratio indicated an increase intracellular influx of Ca^{2+} ions. The addition of AngII is an agonist to intracellular calcium influx. We report that prior exposure of Alport iPSC-PODs to TNF-α for 24 hours had a marked impact on the AngII agonistic effects leading to increased intracellular calcium influx, adversely compared to the WT iPSC-PODs at D10.

CONCLUSIONS

These studies have shown that iPSCs are a valuable *in vitro* model system to study the function of genetic variation. Using iPSC-PODs, we identified TNF-α as a trigger that induces susceptibility of Alport iPSC-derived podocytes to depletion. The chemical chaperone, PBA was found to eliminate morphological aberrations of the RER due to collagen accumulation in Alport G624D iPSC-derived podocytes. iPSC-POD disease modelling and toxicology screening can ultimately enable clinicians to optimize personalized medicine opening up new avenues for affected individuals.

DISCLOSURE

The authors declare no competing interests.

ACKNOWLEDGMENTS

This work was supported by the Alport Foundation of Australia and by grants from the Macquarie/Pedersen Family Trust/Kidney Foundation of Canada/Alport Syndrome Foundation and a European Associations for Information and Research on Kidney Disease Genetic (AIRG) Project Grant.

SUPPLEMENTARY MATERIAL

Supplementary File (PDF)

Figure S1. Generation and characterization of iPSCs using the reprogramming of dermal fibroblasts from X-linked Alport syndrome patients with missense *COL4A5* mutations (PDF)

Figure S2. Calcium imaging after being pre-treated with TNF-α at 20 ng/ml for 24 hours to detect intracellular calcium influx levels activated by AngII in WT and G624D iPSC-PODs D10 (PDF)

Movie S1. Live imaging of G624D iPSC-PODs D10 post TNF-α treatment for a duration of 16 hours (mp4)

Movie S2. Live imaging of G624D iPSC-PODs D10 post TNF-α treatment for a duration of 16 hours (mp4)

Supplementary Methods

Supplementary References

REFERENCES

1. Kruegel J, Rubel D, Gross O. Alport syndrome—insights from basic and clinical research. *Nat Rev Nephrol*. 2013;9:170–178.
2. Ryu M, Kulkarni OP, Radomska E, Miosge N, Gross O, Anders HJ. Bacterial CpG-DNA accelerates Alport glomerulosclerosis by inducing an M1 macrophage phenotype and tumor necrosis factor-α–mediated podocyte loss. *Kidney Int*. 2011;79:189–198.
3. Savige J. Alport syndrome: its effects on the glomerular filtration barrier and implications for future treatment. *J Physiol*. 2017;592:4013–4023.
4. Nijenhuis T, Sloan AJ, Hoenderop JG, et al. Angiotensin II contributes to podocyte injury by increasing TRPC6 expression via an NFAT-mediated positive feedback signaling pathway. *Am J Pathol*. 2011;179:1719–1732.
5. Shankland SJ, Pippin JW, Reiser J, Mundel P. Podocytes in culture: past, present, and future. *Kidney Int*. 2007;72:26–36.
6. Saleem MA, O'Hare MJ, Reiser J, et al. A conditionally immortalized human podocyte cell line demonstrating nephrin and podocin expression. *J Am Soc Nephrol*. 2002;13:630–638.
7. Takahashi K, Tanabe K, Ohnuki M, et al. Induction of pluripotent stem cells from adult human fibroblasts by defined factors. *Cell*. 2007;131:861–872.
8. Lau RW, Wang B, Ricardo SD. Gene editing of stem cells for kidney disease modelling and therapeutic intervention. *Nephrology*. 2018;23:981–990.
9. Song B, Smink AM, Jones CV, Callaghan JM, et al. The directed differentiation of human iPS cells into kidney podocytes. *PLoS One*. 2012;7:e46453.